

Telocyte dynamics in psoriasis

C.G. Manole ^{a, b}, Mihaela Gherghiceanu ^b, Olga Simionescu ^{c, *}

^a Department of Cell Biology and Histology, 'Carol Davila' University of Medicine and Pharmacy, Bucharest, Romania

^b Laboratory of Ultrastructural Research, 'Victor Babeş' National Institute of Pathology, Bucharest, Romania

^c Department of Dermatology, Colentina University Hospital,
'Carol Davila' University of Medicine and Pharmacy, Bucharest, Romania

Received: January 29, 2015; Accepted: April 3, 2015

Abstract

The presence of telocytes (TCs) as distinct interstitial cells was previously documented in human dermis. TCs are interstitial cells completely different than dermal fibroblasts. TCs are interconnected in normal dermis in a 3D network and may be involved in skin homeostasis, remodelling, regeneration and repair. The number, distribution and ultrastructure of TCs were recently shown to be affected in systemic scleroderma. Psoriasis is a common inflammatory skin condition (estimated to affect about 0.1–11.8% of population), a keratinization disorder on a genetic background. In psoriasis, the dermis contribution to pathogenesis is frequently eclipsed by remarkable epidermal phenomena. Because of the particular distribution of TCs around blood vessels, we have investigated TCs in the dermis of patients with psoriasis vulgaris using immunohistochemistry (IHC), immunofluorescence (IF), and transmission electron microscopy (TEM). IHC and IF revealed that CD34/PDGFR α -positive TCs are present in human papillary dermis. More TCs were present in the dermis of uninvolved skin and treated skin than in psoriatic dermis. In uninvolved skin, TEM revealed TCs with typical ultrastructural features being involved in a 3D interstitial network in close vicinity to blood vessels in contact with immunoreactive cells in normal and treated skin. In contrast, the number of TCs was significantly decreased in psoriatic plaque. The remaining TCs demonstrated multiple degenerative features: apoptosis, membrane disintegration, cytoplasm fragmentation and nuclear extrusion. We also found changes in the phenotype of vascular smooth muscle cells in small blood vessels that lost the protective envelope formed by TCs. Therefore, impaired TCs could be a 'missed' trigger for the characteristic vascular pathology in psoriasis. Our data explain the mechanism of Auspitz's sign, the most pathognomonic clinical sign of psoriasis vulgaris. This study offers new insights on the cellularity of psoriatic lesions and we suggest that TCs should be considered new cellular targets in forthcoming therapies.

Keywords: Telocytes • psoriasis • Langerhans cells • dendritic cells • papillary dermis • angiogenesis • Auspitz's sign

Introduction

The cellularity of the dermis is perceived to be comprised of fibroblasts, endothelial cells, pericytes, dendritic cells (DCs), immune cells, macrophages, nerve endings, smooth muscle cells and the recently described telocytes (TCs) [1–3]. TCs are not specific to the dermis (for more details, see www.telocytes.com) and have been described in the interstitium of many organs [4–24]. TCs are characterized by the presence of very long and slender moniform cellular prolongations termed telopodes (Tps). The thickness of the thin segments of Tps (podomers) is comparable to that of collagen fibrils.

The podoms (dilated segments) accommodate mitochondria, endoplasmic reticulum, and caveolae [2, 3, 25]. Recently, the most advanced 3D microscopy technique (FIB-SEM tomography) revealed the spatial conformation of human dermal TCs and their Tps and extracellular vesicles [26]. In human skin, TCs are key components of stem cells niches, where they physically interact with stem cells and other interstitial cells, suggesting an unexplored potential of TCs in skin regeneration and repair [2]. Many studies have showed that TCs are completely different from fibroblasts in terms of cell culture [27, 28], ultrastructure [3, 24, 29, 30], miRNA imprint [31], gene profile [32–34] and proteomics [35].

The involvement of TCs in skin pathology has been shown in scleroderma patients; TCs are numerically reduced in their skin and exhibit numerous ultrastructural particularities, from increased cell volume in the early stage to hallmarks of cellular degeneration in later stages [36–38]. The involvement of TCs in other pathologies has also been reported [39].

*Correspondence to: Olga SIMIONESCU, M.D., Ph.D.,
Department of Dermatology, Colentina University Hospital,
'Carol Davila' University of Medicine and Pharmacy,
Bucharest, Romania.
Tel.: 004 0740 614 342
E-mail: contact@topdermuni.ro

doi: 10.1111/jcmm.12601

© 2015 The Authors.

Journal of Cellular and Molecular Medicine published by John Wiley & Sons Ltd and Foundation for Cellular and Molecular Medicine.

This is an open access article under the terms of the Creative Commons Attribution License, which permits use, distribution and reproduction in any medium, provided the original work is properly cited.

Table 1 The primary antibodies used for the IHC

Antibody	Cell	Dilution	Clone	Producer
CD31	Endothelial cells	1:50	mJC70A	Dako
CD34	Telocytes	1:50	mQBEnd10	Dako
CD117	Melanocytes	1:200	mYR145	Cell Marque, Rocklin, CA, USA
col4	Basal membrane	1:100	mPHM-12	Leica
PDGFRa	Telocytes	1:40	Polyclonal	Neomarkers
S100	Langerhans cells	1:400	Polyclonal	Dako

DCs are cellular participants in the chronic skin inflammatory process that characterizes psoriasis [40–45]. Four subtypes of DCs are known: Langerhans cells (LCs), dermal dendritic cells (DDCs), inflammatory dendritic epidermal cells (iDCs) and plasmacytoid dendritic cells (pDCs); though their specific role(s) are unclear, a notably increased number suggests their involvement in the psoriasis adaptive immune response: [46–49]. Currently, LCs are the most studied type of DC, and their phenotype has been extensively described by immunohistochemical and ultrastructural analysis [50–54]. The rest of the DC subtypes have been immunohistochemically characterized: (i) immature DDCs express CD11c and mature DDCs express CD83 and CD208 (dendritic cells lysosomal associated membrane protein, DC-LAMP) [55]; (ii) iDCs express CD11c, CD14, CD209, nitric oxide synthase (NOS) [43, 56]; and (iii) pDCs express CD11c, CD123, CD205 and TNF α [57–59].

The ability of TCs to establish cellular contacts (either physical or paracrine) with immune cells has been documented in other organs, including skin [2, 3, 25, 29, 36, 60–63]. Thus, in the context of the vast immunology of psoriasis, it is tempting to presume that TCs could be involved in disease initiation and/or progression. Furthermore, (neo-)angiogenesis is at least partially responsible for the clinical signs of psoriasis [64–68]. Previous studies have shown that, within the intense metabolic border zone of myocardial infarction lesions, TCs are involved in neo-angiogenesis, proving their involvement in the reparatory process [69]. Therefore, the involvement of TCs in angiogenesis in psoriasis should be investigated.

In this study we investigated the presence, density and distribution of TCs as a distinct interstitial cell population in the dermis of psoriasis patients. We also assessed whether psoriatic skin TCs exhibit (ultra)structural changes. TCs distribution and the pattern of cellular interaction in psoriasis patients could offer new insights into the pathogenesis and progression of this disease.

Material and methods

Patients

We studied skin samples from 10 patients (5 males and 5 females) with fully developed (mature) plaques of psoriasis vulgaris. Three of the

patients were diagnosed with psoriasis vulgaris type II, and seven were diagnosed with psoriasis vulgaris type I. The triggers of psoriasis were psychological ($n = 8$) or metabolic ($n = 2$). The skin samples were biopsied three times: from the mature psoriatic lesion, non-lesional skin (40 cm distance from any lesion), and after the clearance induced by local treatment. The treatment followed by the patients was entirely topical: keratolytic (urea and salicylic acid) and cyto-reductor (based on Anthraline), followed by calcipotriol and steroid ointments. This study was approved by the Bioethics Committee of the 'Carol Davila' University of Medicine and Pharmacy, Bucharest, according to generally accepted international standards. All subjects provided signed informed consent.

Biopsies

After taking a clinical history and explaining the procedure to the patient, they undressed and the sites of biopsy were chosen. Each of the areas was prepared with a betadine swab to insure sterile conditions. The area was then injected subepidermally with lidocaine HCL 1% (Xilina, Sicomed, Bucharest, Romania) using a 1 ml syringe until a bleb approximately 5 mm diameter formed under the skin. After testing for numbness, the biopsy was performed with a sterile 6 mm skin punch. After the skin was cored and excess blood cleared the fragment of skin, the biopsy was removed using a scalpel and forceps. The post-biopsy lesion was ligated with two stitches of Ethicon Polyglactin 910 (Somerville, NJ, USA). To prevent infection, the wound was dressed with bacitracin Zn and neomycin sulphate powder (Baneocin, Sandoz, Austria) and carefully bandaged.

Each of the skin biopsies were divided into two equal fragments, each fragment following the protocol for paraffin embedding for histology, immunohistochemistry (IHC) and immunofluorescence (IF) or Epon embedding for transmission electron microscopy (TEM).

Histology and immunohistochemistry

Histology and IHC were performed on formalin-fixed, paraffin-embedded, 3- μ m-thick tissue sections made from the tissue samples collected from all patients. For histology, standard haematoxylin and eosin staining was performed. For IHC, samples were incubated with primary antibodies (Table 1) overnight according to standard protocol [20]. We used the Novolink™ Max Polymer Detection System (Leica, New Castle Upon Tyne, UK). Counterstaining was done with haematoxylin, chloralhydrate and lithium carbonate. Images were acquired using a (CCD) AxioCam HRc Zeiss camera with AxioVision software (Carl Zeiss

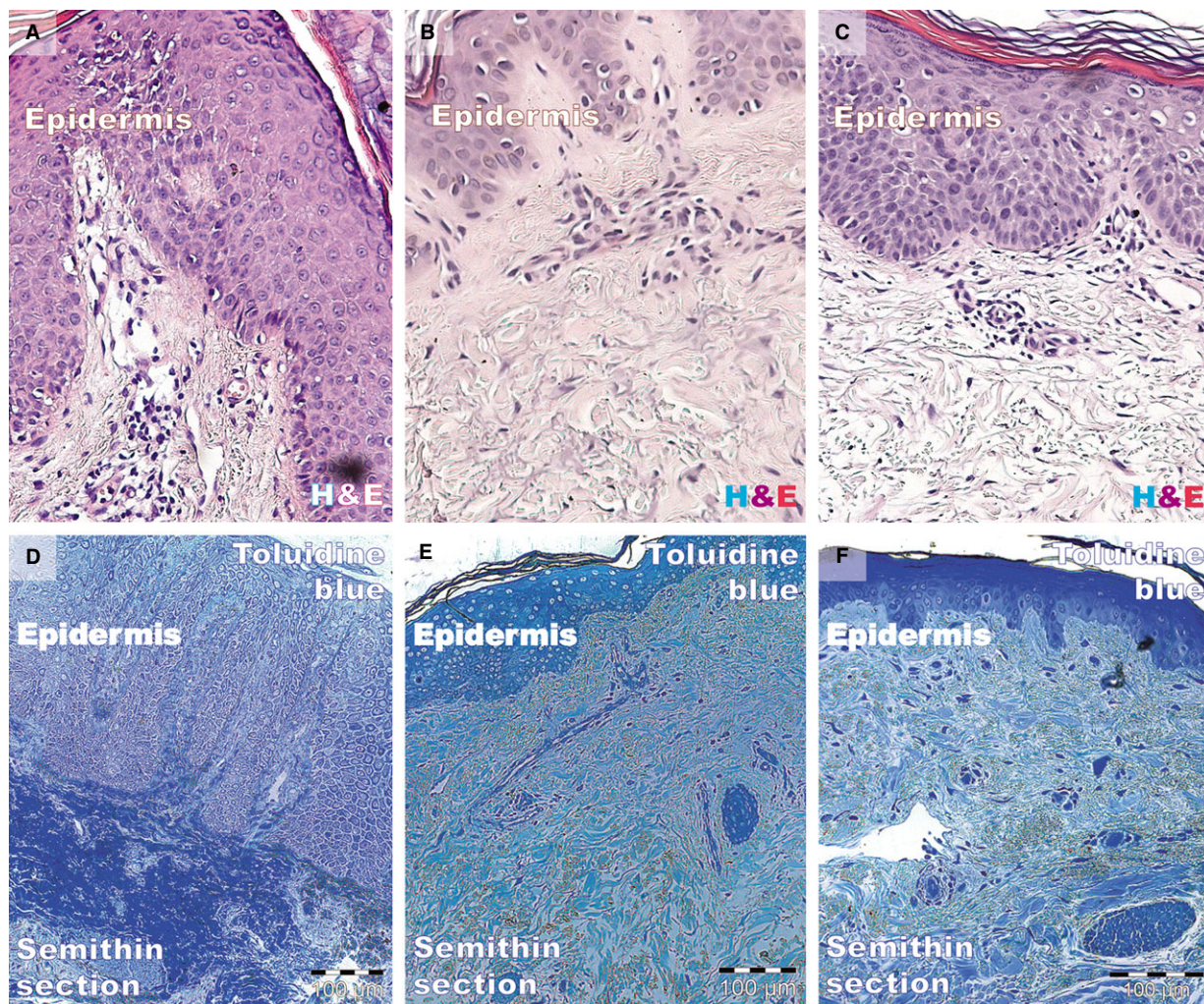


Fig. 1 Light microscopy of paraffin-embedded (A–C, haematoxylin and eosin) and resin-embedded (D–F, toluidine blue) skin biopsies. (A and D) The epidermis of a psoriatic plaque exhibits acanthosis, elongation of rete ridges, and hyperkeratosis with parakeratosis (alternating with orthokeratosis). The papillary dermis is oedematous with dilated blood vessels and inflammatory infiltrate (mainly lymphocytes), which is also in the reticular dermis. (B and E) The epidermis, papillary dermis, and reticular dermis have a normal appearance. (C and F) The thickness of the epidermal layer is similar to that of uninvolved skin. Epithelial cells have a normal appearance in accordance with their position in the epidermis. The dermis is still oedematous but with scarce inflammatory infiltrate. Magnification 200 \times .

Imaging solution GmbH, Oberkochen, Germany) on a Nikon Eclipse E600 microscope (Nikon Instruments Inc., Tokyo, Japan).

Immunofluorescence

For IF we used formalin-fixed paraffin-embedded 3- μ m-thick tissue sections. After deparaffinization, the samples were buffered at 97 $^{\circ}$ C with Epitope Retrieval Solution (Novocastra, Leica) at pH 6 for PDGFR α and pH 9 for CD34. The samples were washed in PBS with glycine (2 mg/ml) and then blocked with 2% BSA for 1 hr. Samples were incubated with primary antibodies overnight at room temperature with a cocktail consisting of mouse monoclonal CD34 (1:50, clone QBEnd10; Dako,

Glostrup, Denmark) and rabbit polyclonal PDGFR α (1:40; Neomarkers, Fremont, CA, USA). After washing three times in EnVisionTM Flex Wash Buffer (Dako) the sections were incubated with anti-mouse Alexa Fluor 488 (1:200; Life Technologies, Molecular Probes, Grand Island, NY, USA) or anti-rabbit rhodamine (1:200; Life Technologies, Molecular Probes) secondary antibodies for another 2 hrs. The nuclei were stained with 4',6-diamidino-2-phenylindole (DAPI; Life Technologies, Molecular Probes). Immunofluorescence studies were performed with a Zeiss Axio Imager Z1 microscope (Carl Zeiss MicroImaging GmbH) using 10 \times , 20 \times , 40 \times , and 63 \times objectives with the appropriate fluorescence filters. Digital images were acquired with a CV-M4+CL CCD camera (JAI, Yokohama, Japan) linked to a computer running the Isis software (Metasystems GmbH, Altlußheim, Germany).

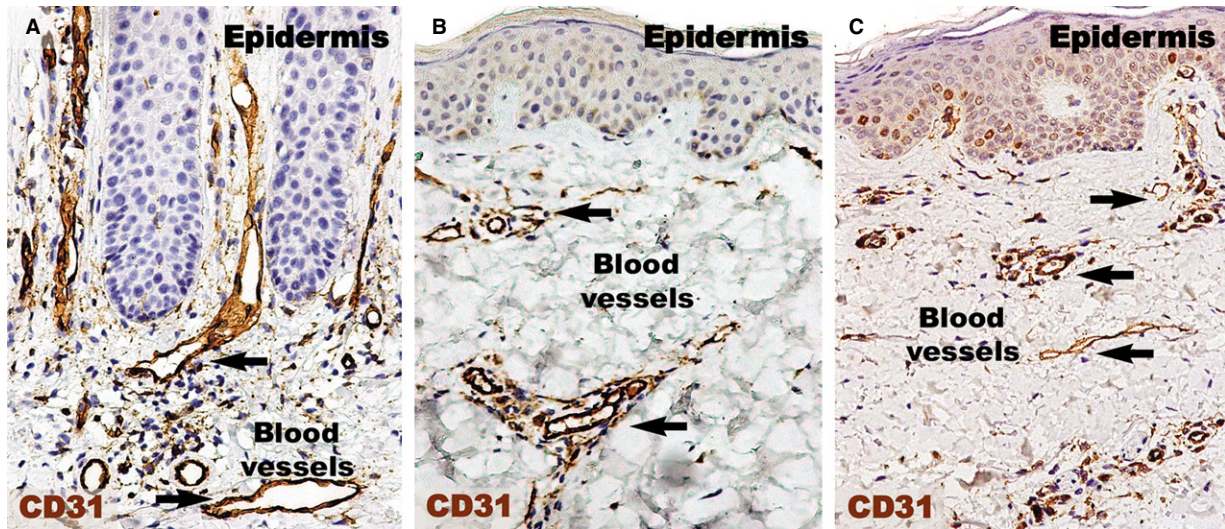


Fig. 2 CD31 immunohistochemistry of a psoriatic plaque (A), distant uninvolved skin (B), and treated skin (C). (A) The density of blood vessels (black arrows) and their diameters are greater in the papillary dermis of a psoriatic plaque compared to uninvolved skin (B). (C) Even if slightly denser, the diameters of blood vessels in the treated skin are comparable to those of uninvolved skin from (B). Magnification 200 \times .

Cell counting

Cell counting was performed on calibrated IF images of known magnification using the NIH ImageJ software [70]. Only cells with DAPI-positive nuclei that presented with positive expression for CD34 (green), PDGFR α (red) or both CD34/PDGFR α (yellow) were considered for the analysis. The counted cells were reported for a total surface of 1 mm². The summation of the surfaces of known magnification images was used to obtain this surface area. Data were processed and statistically analysed using Microsoft Excel software.

Transmission electron microscopy

Transmission electron microscopy was performed on small (1 mm³) tissue fragments processed according to a routine Epon embedding procedure as described previously [2]. Light microscopy was performed on 1 μ m semi-thin sections stained with 1% toluidine blue and digital images recorded using a CCD AxioCam HRc Zeiss camera with AxioVision software (Carl Zeiss Imaging Solution GmbH) on a Nikon Eclipse E600 microscope (Nikon Instruments, Inc.). Thin sections (~60 nm) were examined with a Morgagni 268 transmission microscope (FEI Company, Eindhoven, the Netherlands) at 80 kV. Digital electron micrographs were acquired with a MegaView III CCD and iTEM-SIS software (Olympus, Soft Imaging System GmbH, Münster, Germany). To highlight the TCs and Tps, TEM images were digitally coloured in blue using Adobe[©] Photoshop CS3.

Results

Histology using haematoxylin and eosin and toluidine blue staining is shown in Figure 1. The biopsies taken from fully developed plaques exhibited the hyper-proliferation aspect of psoriasis: acanthosis

(thickening of the epidermis) with characteristic elongation of the rete ridges (tips are clubbed with a tendency to fuse to one another); hyperkeratosis with parakeratosis (alternating with orthokeratosis); and dilated and tortuous blood capillaries in the papillary dermis, with mild oedema, exhibiting chronic inflammatory infiltrate (mainly small lymphocytes). The reticular dermis also contained dilated blood vessels with superficial perivascular infiltration of lymphocytes.

Biopsies from the non-lesional skin showed the normal aspect. Samples from treated patients had decreased epidermal thickness and a smaller rete ridge height. Epithelial cells appeared normal, corresponding to their morphology and staining properties in the epidermal layers. The dermis (papillary or reticular) had decreased inflammatory infiltrate, and the mild oedema was slightly persistent. Eosinophils and neutrophils were absent from the inflammatory infiltrate. In contrast, the distant uninvolved skin and treated lesion had fewer normally matured keratinocyte layers and similar rete ridge lengths.

CD31 expressed (Fig. 2) in the human dermis was increased in the psoriatic plaque compared to distant uninvolved skin. In the psoriatic plaque, the blood vessels were enlarged and had a sinuous trajectory within the papillary dermis. On the other hand, the cellularity around the vessels and CD31 expression was increased. However, we documented a marked reduction in the expression of CD31 in the treated lesions compared to psoriatic lesions, but still higher than in the uninvolved skin. Within the treated psoriatic plaques, CD31-positive endothelial cells were seen in blood vessels in the tips of the dermal papillae.

Endothelial cells were also CD34-positive (Fig. 3). Compared to CD31 positivity, the positive perivascular expression was higher and apparently uniform in the uninvolved skin. Within uninvolved skin dermis, the density of CD34 expression in cellular branched shapes was higher within the adjacent perivascular territory. In psoriatic plaques,

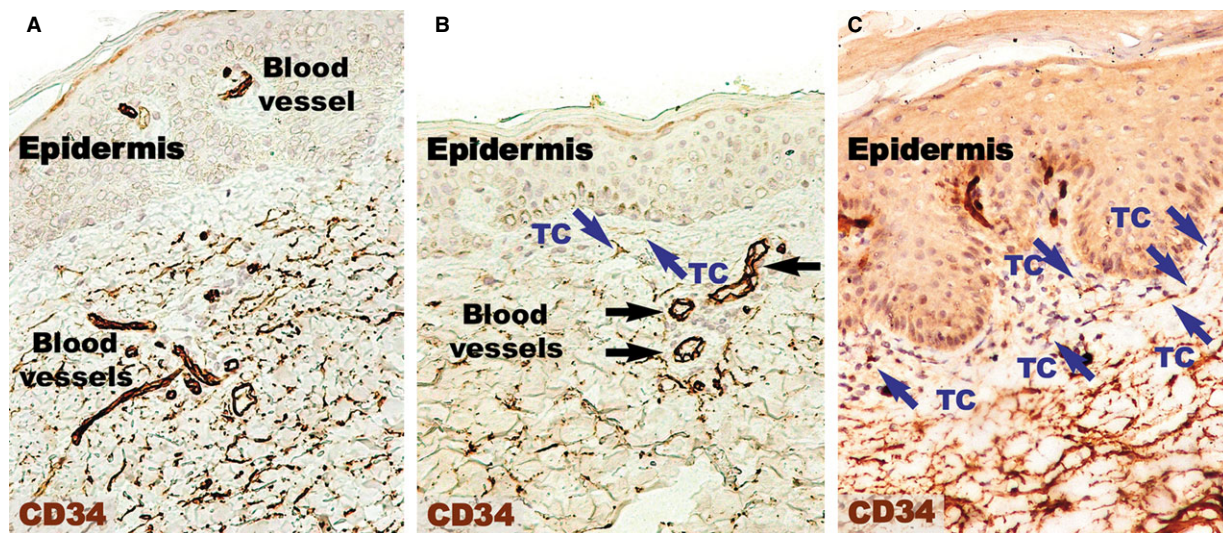


Fig. 3 CD34 immunohistochemistry of a psoriatic plaque (A) revealing a lower density of positive expression in the papillary dermis compared to distant uninvolved skin (B). However, the papillary dermis of treated skin has a density comparable to uninvolved skin (C). CD34 expression is higher within the reticular dermis of psoriatic skin (A) and treated skin (C) compared the reticular dermis of normal skin. Silhouettes of CD34-positive telocytes (TC; blue arrows) with long telopodes were observed in the papillary dermis of normal skin (A) and treated skin (C). Magnification 200 \times . Black arrows indicate blood vessels.

CD34 was uniformly increased in the reticular dermis. The papillary dermis seemed to lack CD34-positive structures.

Higher magnifications (Fig. 4) of distant uninvolved skin revealed CD34-positive cells in a fusiform silhouette with very long cellular prolongations. These interstitial cells are distinct from endothelial cells and specifically located in close proximity of blood vessels within the papillary dermis. Such CD34-positive cells are not present near the dilated capillaries in the dermis of psoriatic plaques. In the treated lesional skin, the general expression of CD34 was slightly increased compared to uninvolved skin. Fusiform cells were present in the papillary dermis, parallel and in close proximity to the basement

membrane. Moreover, these cells were situated in the proximity of blood vessels.

PDGFR α -positive cells (Fig. 5) were present in the papillary dermis of distant uninvolved skin. These elongated cells with very long cellular prolongations were situated below the basement membrane and ran parallel to the basement membrane. These cells were also found close and/or enwrapping the blood vessels. The reaction for PDGFR α was increased in the papillary dermis of the lesional dermis, probably in the context of the chronic inflammation that characterizes psoriasis. However, no visible PDGFR α fusiform cells were found in the dermis. The healing process resulted in increased positivity for

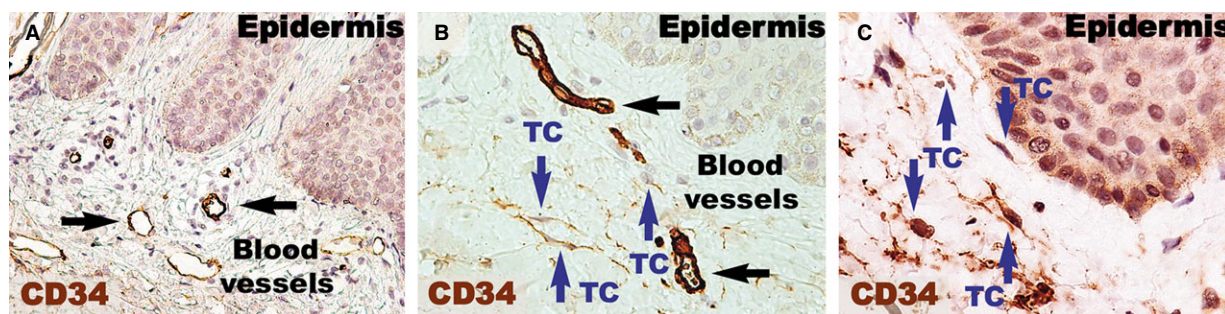


Fig. 4 CD34 immunohistochemistry reveals reduced expression in the papillary dermis of a psoriatic plaque (A) compared to the papillary dermis of distant uninvolved skin (B) and treated skin (C). (A) The blood vessels are more numerous and dilated in the psoriatic plaque dermis compared to (B and C). Also, no CD34 positivity was found in interstitial cells in the papillary dermis. (B) In the papillary dermis of uninvolved skin, telocytes (TC; blue arrows) appear positive for CD34 in the vicinity of blood vessels. (C) The presence of CD34-positive telocytes (TC; blue arrows) was also noted in the papillary dermis of treated skin, with telopodes running parallel to the basement membrane of the epidermis. Black arrows indicate blood vessels. Magnification 400 \times .

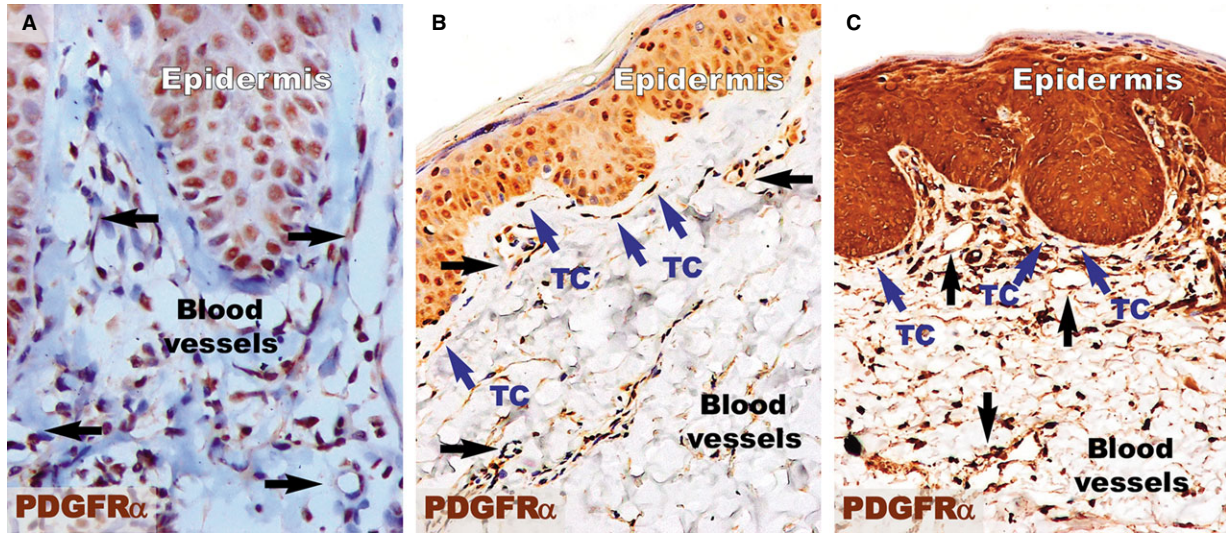


Fig. 5 PDGFR α immunohistochemistry revealed an increased density of PDGFR α -positive structures in the papillary dermis of a psoriatic plaque (A) and treated skin (C) compared to the papillary dermis of distant uninvolved skin (B). (A) The papillary dermis of the lesional skin has increased cellularity, but no PDGFR α -positive telocytes were observed. Blood vessels (black arrows) have dilated diameters within the dermis. (B) Telocytes (TC; blue arrows) positive for PDGFR α are seen in the papillary dermis of uninvolved skin. TCs have very long prolongations that run parallel to the basement membrane of the epidermis. (C) PDGFR α -positive telocytes (TC; blue arrows) are observed among the increased cellularity of the papillary dermis of treated skin and have the same orientation as in uninvolved skin. The blood vessels have comparable diameters to those in uninvolved skin. Black arrows indicate blood vessels. Magnification 200 \times .

PDGFR α within the papillary dermis. Higher magnifications (Fig. 6) revealed the presence of elongated cells in the papillary dermis, close to the basement membrane. The cellular processes were very long

and moniliform. Such cells were absent in the psoriatic papillary dermis, but they were also found in treated psoriatic skin lesions, bordering the basement membrane.

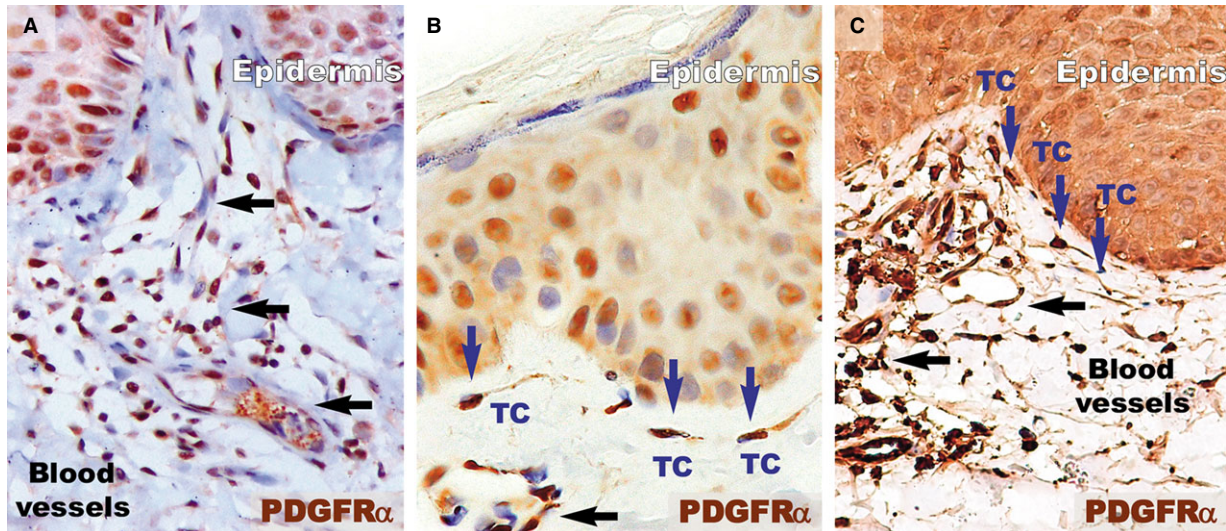


Fig. 6 Higher magnifications of immunohistochemistry for PDGFR α in the papillary dermis show the absence of telocytes but the presence of inflammatory cells (mainly lymphocytes) in a psoriatic plaque (A). However, in the distant uninvolved skin (B), telocytes (TC, blue arrows) with very long telopodes are situated in the papillary dermis and run parallel to the line of the dermal-epidermal junction. (C) Telocytes (TC; blue arrows) were also observed in the papillary dermis of treated skin, with their telopodes running parallel to the basement membrane. Black arrows indicate blood vessels. Magnification 400 \times .

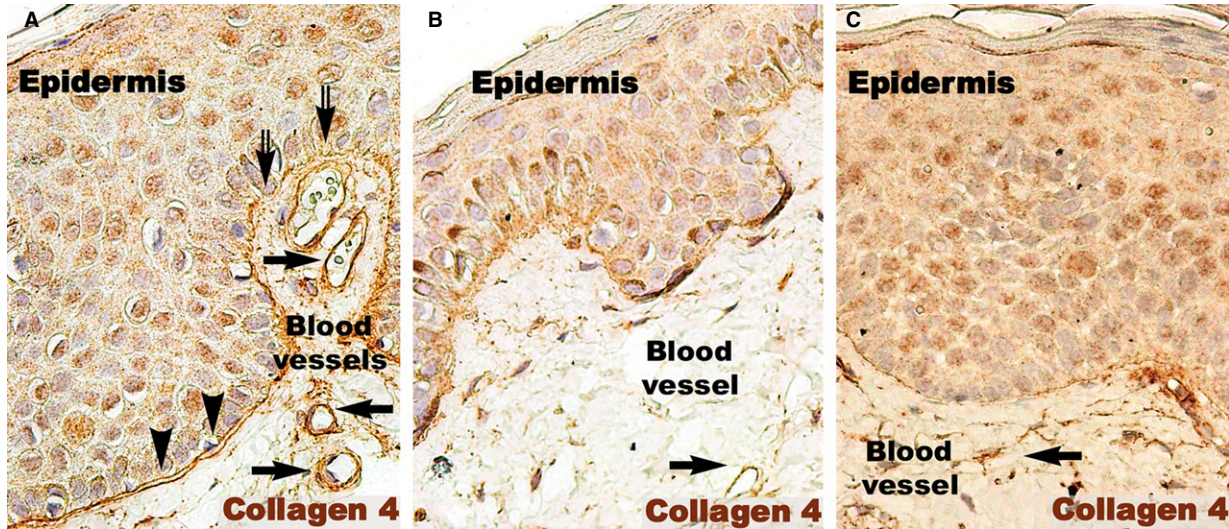


Fig. 7 Collagen 4 immunohistochemistry of a psoriatic plaque (A), distant uninvolved skin (B), and treated skin (C). (A) Immunohistochemistry revealed the bi-layer aspect of the basal membrane in the psoriatic plaque (arrow heads). Focally, the continuity of the basal membrane was interrupted (double arrows). This aspect is different from the single line continuum of the distant uninvolved skin (B) and treated skin (C). Black arrows indicate blood vessels. Magnification 200 \times .

The basement membrane appeared mostly as a continuous layer in IHC for col-4, but foci of discontinuity were observed in active psoriatic lesions (Fig. 7A). The basal cells of the epidermis seemed to protrude into the loose connective tissue of the papillary dermis. Moreover, the basement membrane had segments with a stratified appearance and visible space between sublayers.

The space between keratinocytes in the basal and supra-basal layers seemed to be increased. As in the case of non-lesional skin, treated lesions had a continuous basement membrane (Fig. 7B and C).

The number of S100-positive cells (Fig. 8) was not different in psoriatic skin and distant uninvolved skin. However, in the psoriatic

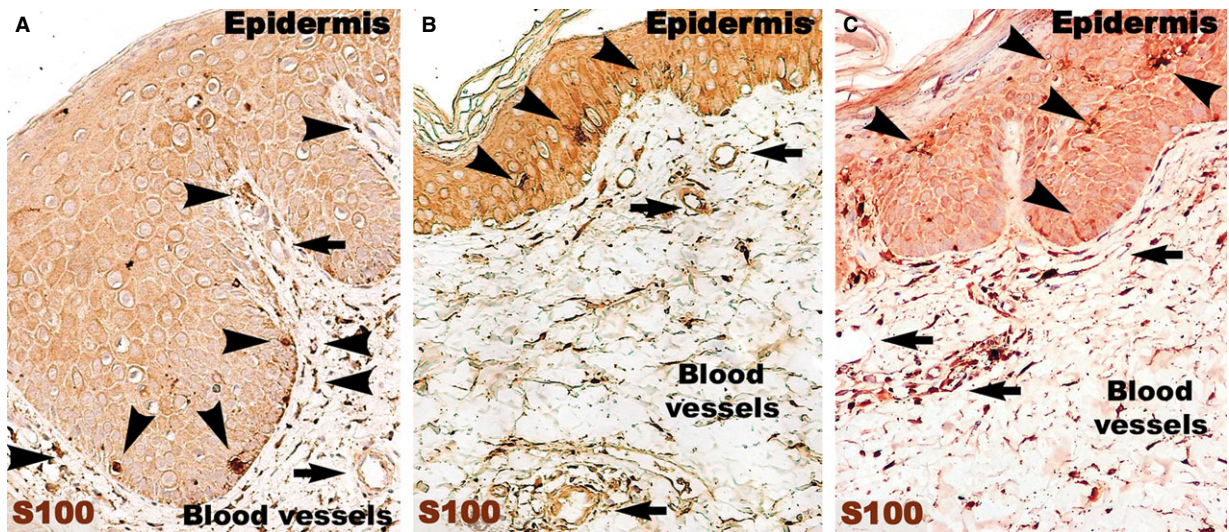


Fig. 8 S100 immunohistochemistry of a psoriatic plaque (A) reveals an increased density of S100-positive Langerhans cells (arrow heads) beneath the basal membrane of the epidermis, and just a few positive Langerhans cells in the epidermis. In both distant uninvolved skin (B) and treated skin (C), S100-positive Langerhans cells (arrow heads) are situated in the epidermis. Black arrows indicate blood vessels. Magnification 200 \times .

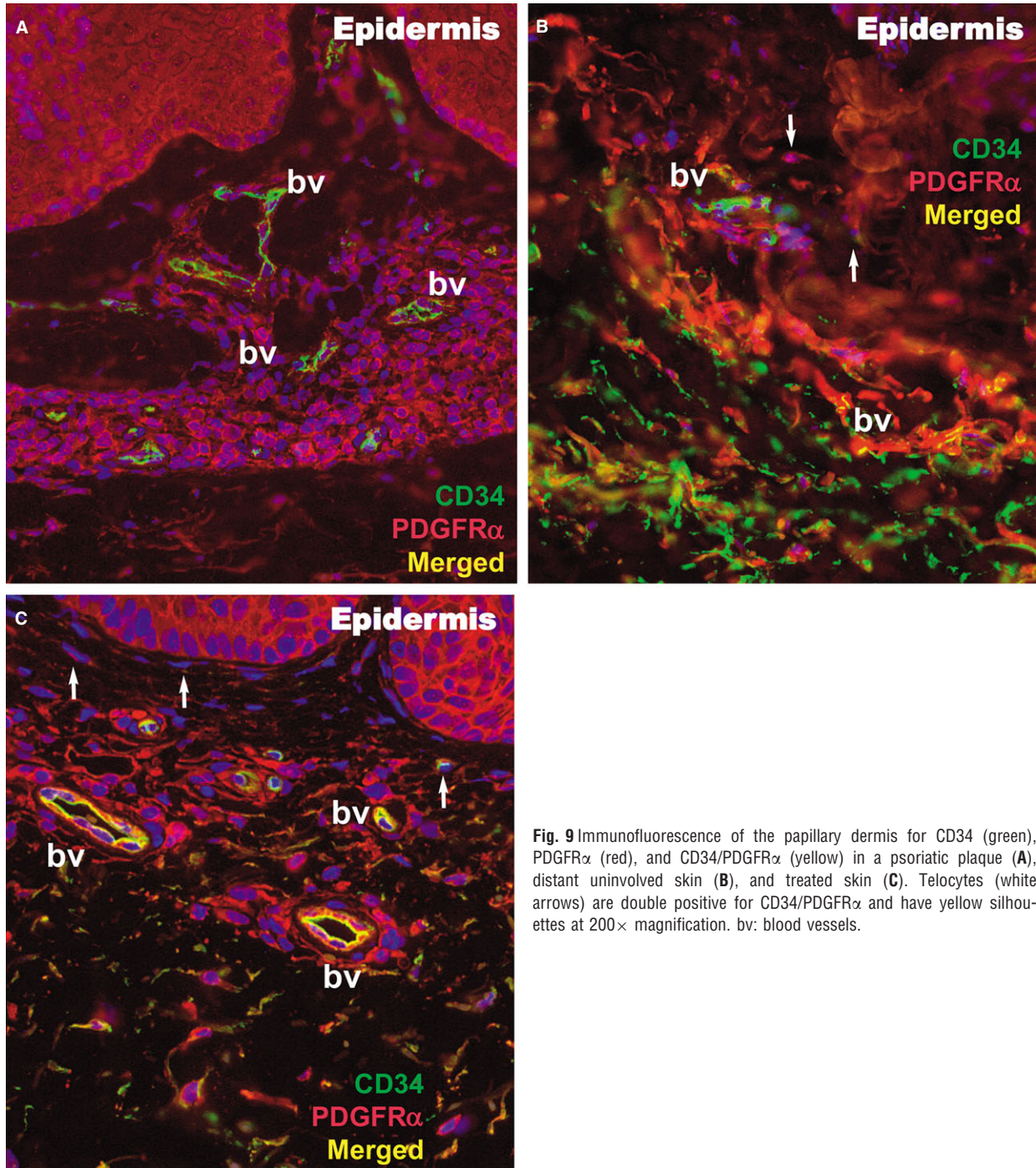


Fig. 9 Immunofluorescence of the papillary dermis for CD34 (green), PDGFR α (red), and CD34/PDGFR α (yellow) in a psoriatic plaque (**A**), distant uninvolved skin (**B**), and treated skin (**C**). Telocytes (white arrows) are double positive for CD34/PDGFR α and have yellow silhouettes at 200 \times magnification. bv: blood vessels.

skin, the S100-positive cells were predominantly situated in the papillary dermis among the basal cells of the epidermis. In contrast, the uninvolved skin had S100-positive DCs in the supra-basal layers of epidermis. In treated skin, S100-positive cells were also found in the entire thickness of the epidermis.

Within the papillary and reticular dermis of uninvolved skin, IF for CD34 and PDGFR α revealed multiple double-positive cells (Fig. 9). The appearance of these CD34/PDGFR α -positive cells is indicative of TCs, presenting a small cell body and very long prolongations at high magnifications. The density of these cells

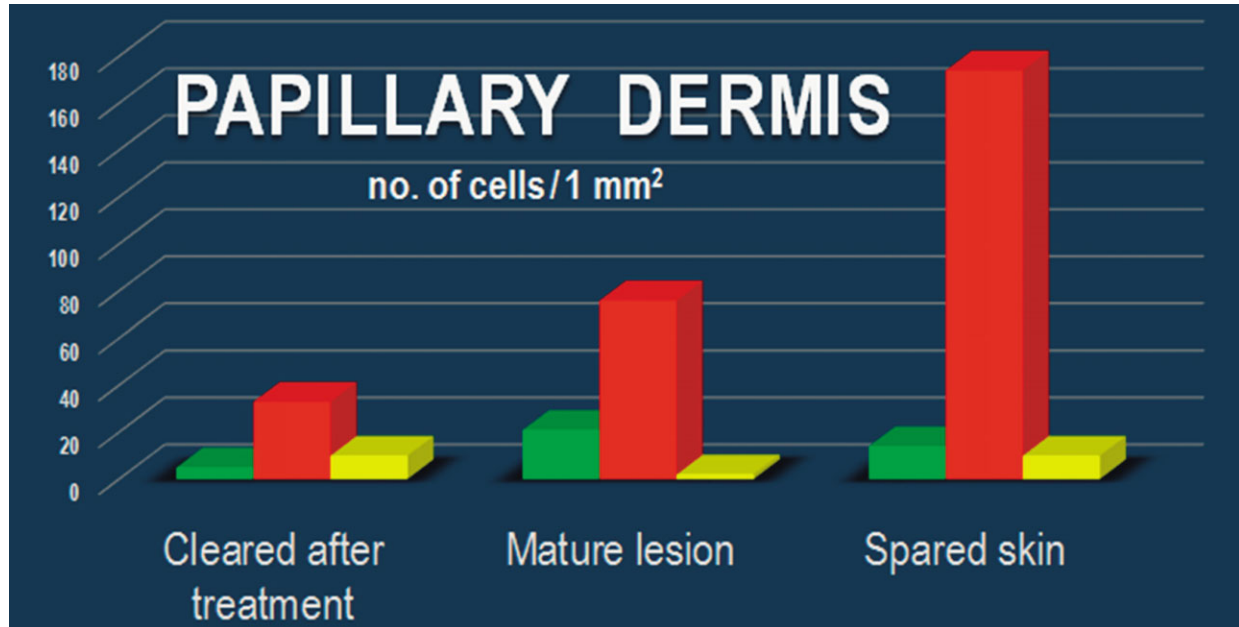


Fig. 10 Dynamics of the number of CD34⁺ cells, PDGFR α ⁺ cells, and CD34⁺/PDGFR α ⁺ cells in the dermis of uninvolved skin (A), lesional skin (B), and treated skin (C).

calculated on IF images of the papillary dermis was 10 cells/mm² (Fig. 10).

In the lesional reticular dermis, the measured density of CD34/PDGFR α -positive cells was comparable to that of the non-lesional reticular dermis (Fig. 10), but in the lesional papillary dermis it was decreased (Fig. 10). In both sublayers of the dermis, the general positivity for PDGFR α was increased in cells belonging to different structures. This could be perceived in the context of the extensive inflammatory process and substantial angiogenesis documented by IHC (Figs 2 and 3). The endothelial cells positive for CD34 in dilated blood vessels were observed in both papillary and reticular dermis.

Both papillary and reticular dermis in treated skin had a considerable decrease in general positivity for PDGFR α . Interstitial cells expressing double CD34/PDGFR α positivity were also observed (Figs 9 and 10). Their particular conformation with long cellular prolongations emerging from a small cell body was suggestive of TCs (Fig. 9). The density of CD34/PDGFR α double-positive interstitial cells in treated skin was similar to that of uninvolved papillary dermis, but it was increased in the reticular dermis (Fig. 10).

Transmission electron microscopy analyses focused on the connective tissue of the papillary dermis with an emphasis on TCs. TCs were identified based on their characteristic ultrastructural morphology as interstitial cells with long cellular processes (Fig. 11A). TCs with normal morphology were frequently present in non-lesional skin (Fig. 11A) but rare in the papillary and reticular dermis from psoriatic skin (Fig. 11B and C). Moreover, the TCs exhibited degenerative ultrastructural features in psoriatic skin

(Figs 11B, C and 12). Transmission electron microscopy revealed TCs with apoptotic nuclei (Fig. 11C), dystrophic TCs with fragmented Tps (Fig. 11B), and TCs with nuclear extrusions and cytoplasmic disintegration (Fig. 12A) in psoriatic lesions. We found no homocellular contacts between TCs in psoriatic skin. Extruded nuclei (Fig. 12B) or apoptotic TCs (Fig. 11C) were often observed to have close contacts with DCs in the dermis of psoriatic skin.

DCs were frequently detected in psoriatic plaques and identified by TEM based on their morphology as cells with a stellate or tree-like appearance and numerous fine processes (Figs 11C and 13). Among DCs known to be present in psoriatic lesions, LCs and pDCs were identified because of their characteristic ultrastructural features of Birbeck granules (Fig. 13A and B) and abundant rough endoplasmic reticulum respectively (Fig. 13C). LCs migrated from the epidermis to the dermis through the broken basement membrane (Fig. 13A) and were observed in the papillary dermis (Fig. 13B). The epidermal-dermal basement membrane in psoriatic plaques often showed breaks (Figs 11B and 13A) with col-4 staining (Fig. 7) but was continuous in non-lesional skin.

Ultrastructural changes were visible on vascular smooth muscle cells (VSMCs) in small blood vessels in psoriatic skin (Fig. 14). In addition to the normal contractile phenotype of VSMCs (Fig. 14A), the cells often exhibited a synthetic phenotype with decreased actin filaments and increased rough endoplasmic reticulum (Fig. 14B and C). The VSMCs with a synthetic phenotype were hypertrophic (Fig. 14B) or atrophic (Fig. 14C) and had loose connections with endothelial cells (Fig. 14C). Notably, the blood vessels containing VSMCs with the synthetic phenotype were not surrounded by TCs (Fig. 14B and C).

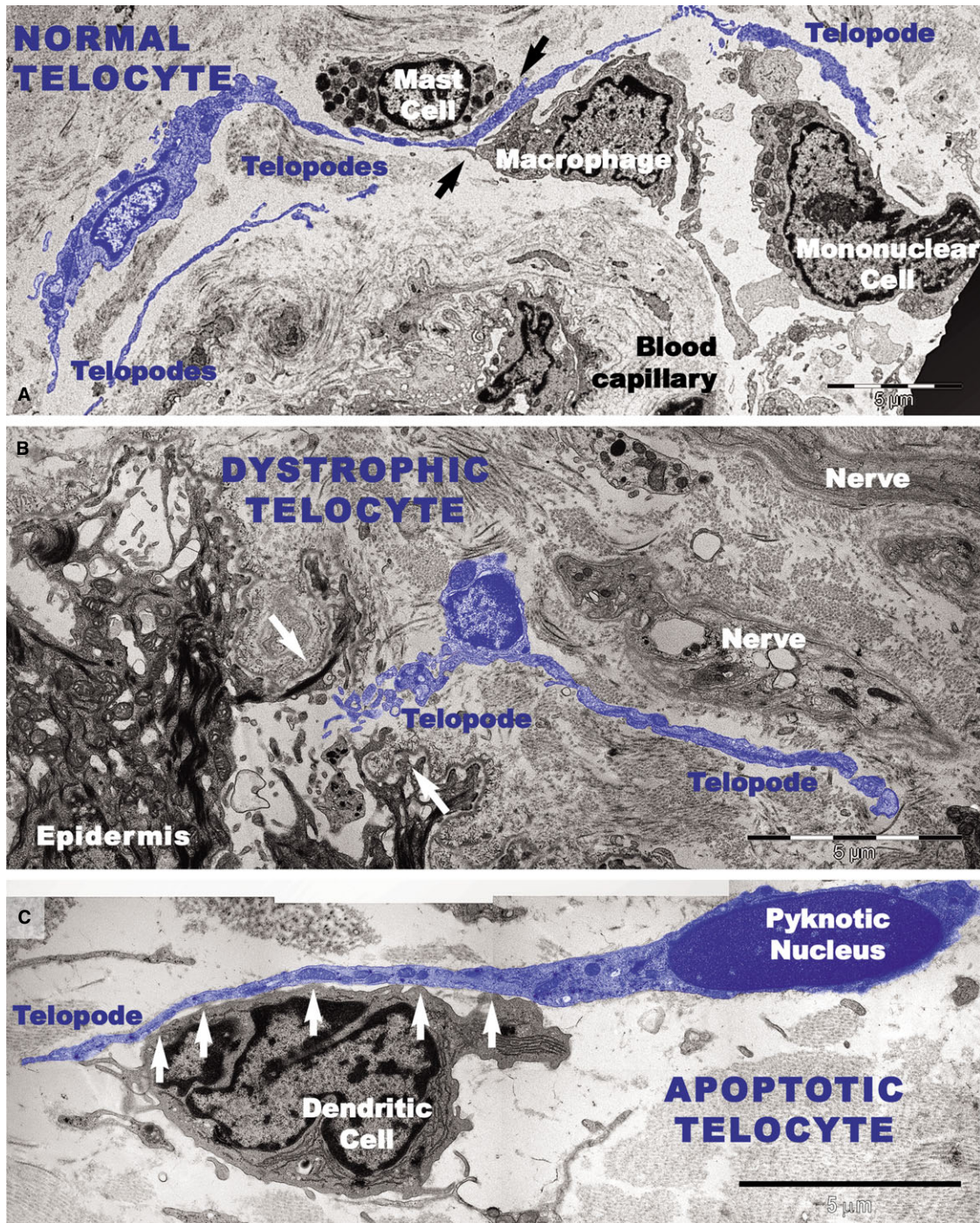


Fig. 11 Digitally coloured transmission electron microscope images highlight telocytes in blue. **(A)** A telocyte with long telopode alongside a mast cell, a macrophage, and a mononuclear cell surrounding a blood vessel in uninvolved skin. Close contacts between telocytes and mast cells and between telocytes and macrophages are visible (black arrows). **(B and C)** TEM shows altered morphology of telocytes in the papillary dermis of a psoriatic plaque. **(B)** A telocyte with reduced perinuclear cytoplasm is visible beneath the epidermis at the site of a broken (white arrows) basement membrane. **(C)** An apoptotic telocyte with condensed chromatin in the nucleus has close contacts (white arrows) with a dendritic cell in the dermis of a psoriatic plaque. The dendritic cell has short processes.

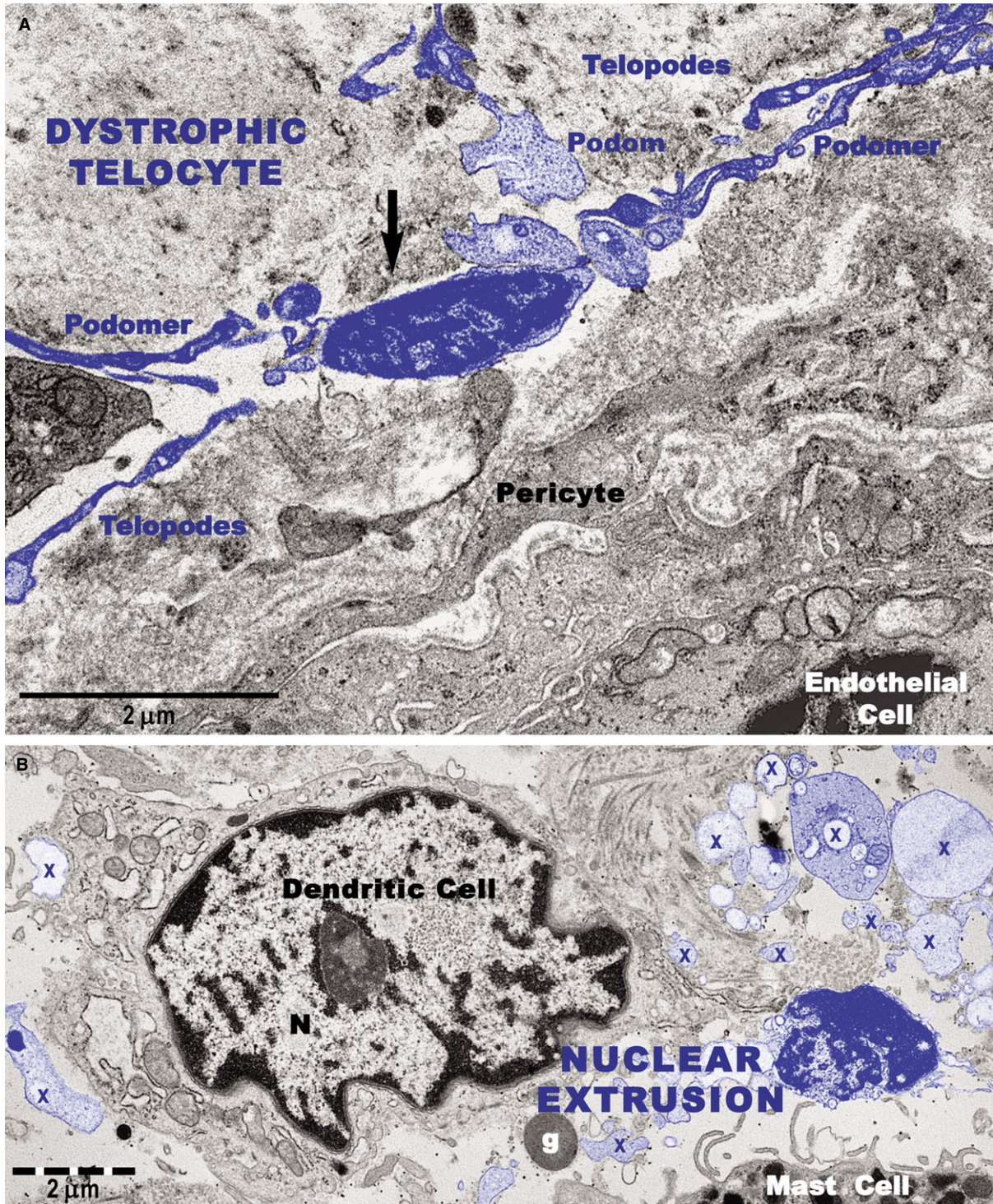


Fig. 12 Transmission electron microscope images show degenerative changes in telocytes (digitally coloured in blue) from a psoriatic plaque. **(A)** A telocyte with shrivelled nucleus and detached telopodes. The arrow indicates dissolution of the cellular membrane and the cytoplasmic content surrounding the nucleus. **(B)** An extruded nucleus and cytoplasmic fragments (X) of a telocyte are visible in the vicinity of a dendritic cell. g: granule (of a mast cell).

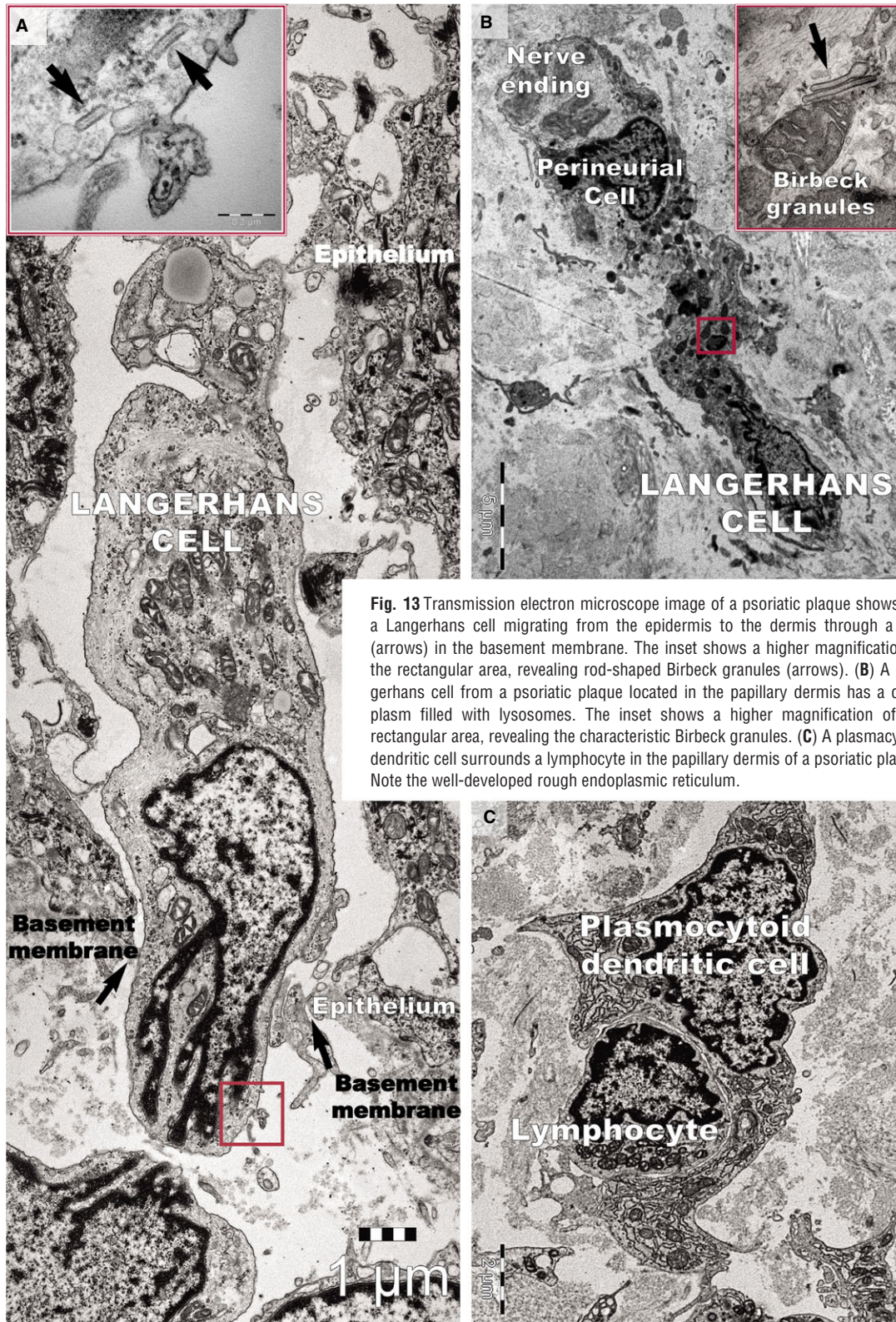


Fig. 13 Transmission electron microscope image of a psoriatic plaque shows (A) a Langerhans cell migrating from the epidermis to the dermis through a gap (arrows) in the basement membrane. The inset shows a higher magnification of the rectangular area, revealing rod-shaped Birbeck granules (arrows). (B) A Langerhans cell from a psoriatic plaque located in the papillary dermis has a cytoplasm filled with lysosomes. The inset shows a higher magnification of the rectangular area, revealing the characteristic Birbeck granules. (C) A plasmacytoid dendritic cell surrounds a lymphocyte in the papillary dermis of a psoriatic plaque. Note the well-developed rough endoplasmic reticulum.

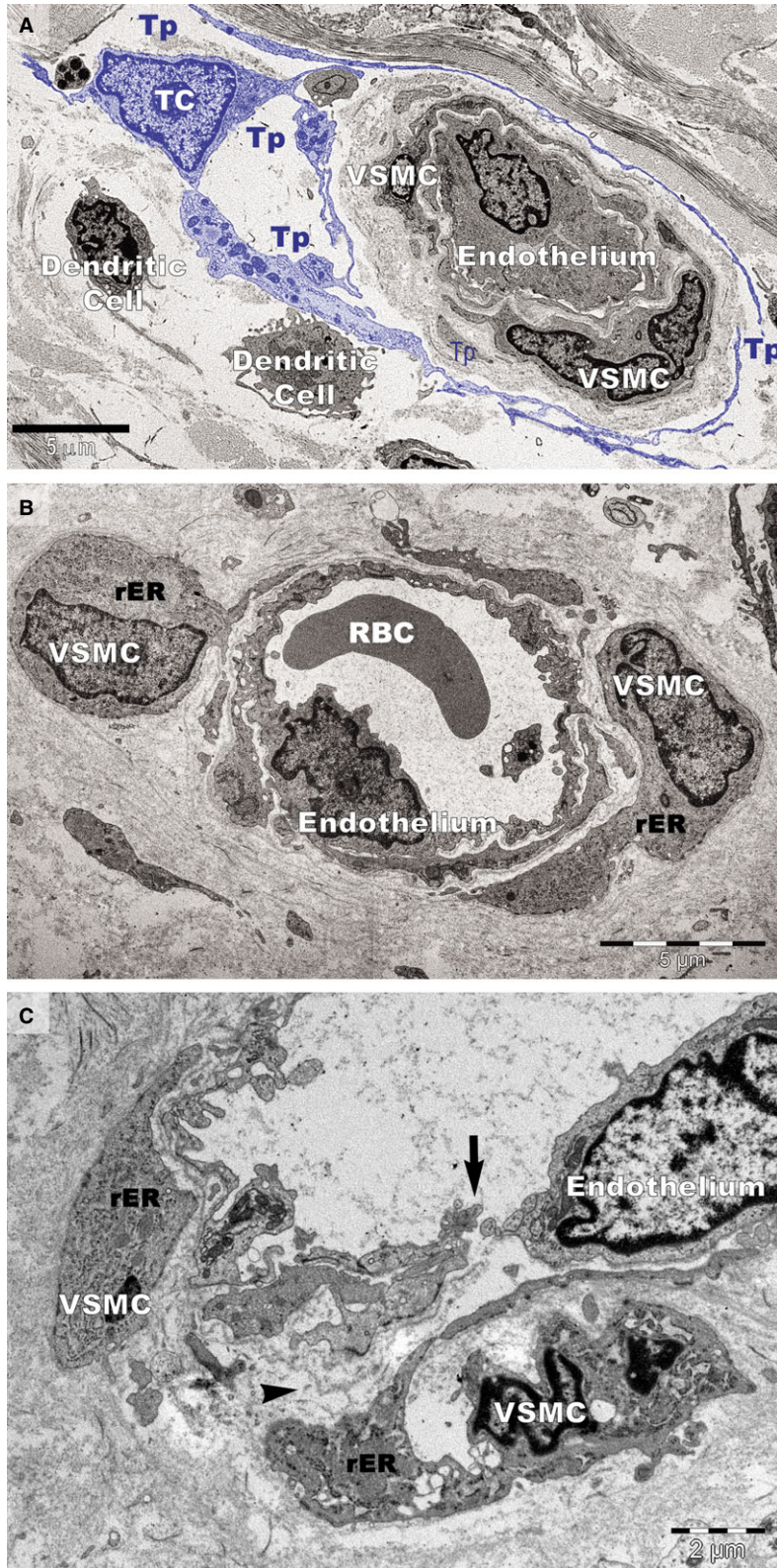


Fig. 14 Transmission electron microscopy of small blood vessels in psoriatic plaques. **(A)** Vascular smooth muscle cell (VSMC) of contractile phenotype is visible in a terminal arteriole surrounded by the telopodes (Tp) of a telocyte (TC; digitally coloured in blue). Dendritic cells have short processes. **(B)** VSMCs with abundant rough endoplasmic reticulum (rER) in the cytoplasm are bulging into the perivascular space (hypertrophy). RBC: red blood cell. **(C)** VSMCs of synthetic phenotype in a terminal arteriole are detached from the endothelial layer. A gap (arrow) is visible between endothelial cells that lost their junctions. The basement membrane of the endothelium is also discontinuous (arrowhead).

Discussion

The pathogenesis of psoriasis is not fully understood despite efforts to focus on cellular types and signalling molecules [44, 55]. Here, we investigated the dynamics of TCs in the vulgar form of psoriasis. As TCs are thought to be key players in the regulation of tissue/organ homeostasis [2], our data suggest that TC loss may have important pathophysiological implications in psoriasis.

We found a decreased number of TCs in psoriatic papillary dermis and observed their recovery after local corticoid therapy. Immunofluorescence showed that the density of TCs identified as CD34/PDGFR α -positive cells was comparable in the dermis of uninvolved and treated skin but decreased in the lesional papillary dermis. Electron microscopy showed that TCs undergo apoptosis and dystrophic changes in psoriatic plaques. Also, IHC showed that CD34-positive cells are not present near dilated capillaries in the dermis of psoriatic plaques. Notably, the interstitial expression of CD34 was slightly increased in the proximity of blood vessels in treated lesional skin. These data suggest TC recovery after topic corticoid therapy despite the residual inflammatory microenvironment [44].

We found that TCs usually surround blood vessels in normal skin [2]. This study shows noticeable changes in the phenotype of VSMCs in small blood vessels that are not surrounded by TCs in the papillary dermis of psoriatic skin. The tortuous, widened, elongated capillaries seem to play a central role in the pathogenesis of psoriasis [71], and endothelial cell gaps in psoriatic vessels have been reported [72], but we found no information on VSMC phenotype changes or the involvement of adventitial cells usually referred to as veil cells [72].

The 3D reconstruction of dermal TCs by FIB-SEM tomography revealed various conformations of Tps: long, flattened irregular veils (ribbon-like segments) and tubular structures (podomers) with uneven calibre because of irregular dilations (podoms) [26]. This 3D appearance of TCs is similar to that of 'veil cells' described in the skin [72]. The exact nature and function of these cells are still undetermined considering they lack cell markers for T, B, LCs, or HLA-DR [72].

Vasodilatation tests indicated that arterioles in psoriatic plaques are not normally maximally dilated but have a basal constrictor tone

[73]. Loss of the contractile phenotype of VSMCs in arterioles from plaques could cause the phenotype change in VSMCs and, consequently, the structural widening of arterioles. Studies have shown that phenotype alterations and differentiation of VSMCs are important for angiogenesis, blood vessel remodelling and homeostasis, and both the composition and organization of the extracellular matrix (ECM) have major consequences for the smooth muscle cell phenotype [74, 75]. Preferential distribution of TCs around blood vessels could be important in vascular physiology, and TCs certainly contribute to the composition and organization of the ECM. The loss of perivascular TCs could trigger the characteristic vascular pathology in psoriasis. Moreover, the loss of TCs could be considered a mechanism underlying the most pathognomonic sign of psoriasis vulgaris, Auspitz's sign.

We previously showed that, within the dermis, TCs form an interstitial network based on homocellular (TC-TC junctions) and heterocellular (TC-other interstitial cells) interactions, suggesting an essential role of TCs in intercellular signalling required for skin homeostasis [2]. Recent studies have shown that TC injury may have important pathophysiological implications in systemic sclerosis [36, 37]. The loss of TCs and their interstitial network may significantly influence psoriatic lesion initiation and/or pathology progression, impairing long distance heterocellular communication.

In conclusion, damaged TCs could be an important step in the pathophysiology of psoriasis. This study offers new insights into the cellularity of psoriatic lesions and we suggest considering TCs as new cellular targets for forthcoming therapies. Because pustular psoriasis is not characterized by Auspitz's sign, clarifying the involvement of TCs in other forms of psoriasis would be attractive. In the future, we propose extending the research to the pustular and erythrodermic forms of psoriasis.

Acknowledgements

This work was supported by a grant from the Romanian National Authority for Scientific Research, project number PN 09.33N/2009 [MG] and partly supported by the Sectorial Operational Programme for Human Resources Development (SOPHRD), financed by the European Social Fund and the Romanian Government under contract number POSDRU 159/1.5/S/141531 [CGM].

References

1. **Prost-Squarcioni C, Freitag S, Heller M, et al.** Functional histology of dermis. *Ann Dermatol Venereol.* 2008; 135: 1S5–20.
2. **Ceafalan L, Gherghiceanu M, Popescu LM, et al.** Telocytes in human skin - are they involved in skin regeneration? *J Cell Mol Med.* 2012; 16: 1405–20.
3. **Cretoiu SM, Popescu LM.** Telocytes revisited. *Biomol Concepts.* 2014; 5: 353–69.
4. **Zhao B, Liao Z, Chen S, et al.** Intramyocardial transplantation of cardiac telocytes decreases myocardial infarction and improves post-infarcted cardiac function in rats. *J Cell Mol Med.* 2014; 18: 780–9.
5. **Yang Y, Sun W, Wu SM, et al.** Telocytes in human heart valves. *J Cell Mol Med.* 2014; 18: 759–65.
6. **Edelstein L, Smythies J.** The role of telocytes in morphogenetic bioelectrical signaling: once more unto the breach. *Front Mol Neurosci.* 2014; 7: 41.
7. **Galiger C, Kostin S, Golec A, et al.** Phenotypical and ultrastructural features of Oct4-positive cells in the adult mouse lung. *J Cell Mol Med.* 2014; 18: 1321–33.
8. **Li H, Lu S, Liu H, et al.** Scanning electron microscope evidence of telocytes in vasculature. *J Cell Mol Med.* 2014; 18: 1486–9.
9. **Li H, Zhang H, Yang L, et al.** Telocytes in mice bone marrow: electron microscope evidence. *J Cell Mol Med.* 2014; 18: 975–8.
10. **Wang F, Song Y, Bei Y, et al.** Telocytes in liver regeneration: possible roles. *J Cell Mol Med.* 2014; 18: 1720–6.
11. **Vannucchi MG, Traini C, Guasti D, et al.** Telocytes subtypes in human urinary bladder. *J Cell Mol Med.* 2014; 18: 2000–8.

12. **Díaz-Flores L, Gutiérrez R, García MP, et al.** Uptake and intracytoplasmic storage of pigmented particles by human CD34⁺ stromal cells/telocytes: endocytic property of telocytes. *J Cell Mol Med.* 2014; 18: 2478–87.
13. **Manetti M, Rosa I, Messerini L, et al.** Telocytes are reduced during fibrotic remodelling of the colonic wall in ulcerative colitis. *J Cell Mol Med.* 2015; 19: 62–73.
14. **Díaz-Flores L, Gutiérrez R, García MP, et al.** Human resident CD34⁺ stromal cells/telocytes have progenitor capacity and are a source of α uma⁺ cells during repair. *Histol Histopathol.* 2014. In press.
15. **Bosco C, Díaz E, Gutiérrez R, et al.** Placental hypoxia developed during preeclampsia induces telocytes apoptosis in chorionic villi affecting the maternal-fetus metabolic exchange. *Curr Stem Cell Res Ther.* 2015. DOI: 10.2174/1574888X10666150202144855
16. **Fu S, Wang F, Cao Y, et al.** Telocytes in human liver fibrosis. *J Cell Mol Med.* 2015; 19: 676–83.
17. **Roatesi I, Radu BM, Cretoiu D, et al.** Uterine telocytes: a review of current knowledge. *Biol Reprod.* 2015. doi:10.1095/biolreprod.114.125906.
18. **Díaz-Flores L, Gutiérrez R, Sáez FJ, et al.** Telocytes in neuromuscular spindles. *J Cell Mol Med.* 2013; 17: 457–65.
19. **Niculite CM, Regalia TM, Gherghiceanu M, et al.** Dynamics of telopodes (telocyte prolongations) in cell culture depends on extracellular matrix protein. *Mol Cell Biochem.* 2015; 398: 157–64.
20. **Cretoiu SM, Radu BM, Banciu A, et al.** Isolated human uterine telocytes: immunocytochemistry and electrophysiology of T-type calcium channels. *Histochem Cell Biol.* 2015; 143: 83–94.
21. **Luesma MJ, Gherghiceanu M, Popescu LM.** Telocytes and stem cells in limbus and uvea of mouse eye. *J Cell Mol Med.* 2013; 17: 1016–24.
22. **Cretoiu D, Hummel E, Zimmermann H, et al.** Human cardiac telocytes: 3D imaging by FIB-SEM tomography. *J Cell Mol Med.* 2014; 18: 2157–64.
23. **Fertig ET, Gherghiceanu M, Popescu LM.** Extracellular vesicles release by cardiac telocytes: electron microscopy and electron tomography. *J Cell Mol Med.* 2014; 18: 1938–43.
24. **Popescu LM, Curici A, Wang E, et al.** Telocytes and putative stem cells in ageing human heart. *J Cell Mol Med.* 2015; 19: 31–45.
25. **Popescu LM, Faussonne-Pellegrini MS.** TELECYTES - a case of serendipity: the winding way from Interstitial Cells of Cajal (ICC), via Interstitial Cajal-Like Cells (ICLC) to TELECYTES. *J Cell Mol Med.* 2010; 14: 729–40.
26. **Cretoiu D, Gherghiceanu M, Hummel E, et al.** FIB-SEM tomography of human skin telocytes and their extracellular vesicles. *J Cell Mol Med.* 2015; 19: 714–22.
27. **Sheng J, Shim W, Lu J, et al.** Electrophysiology of human cardiac atrial and ventricular telocytes. *J Cell Mol Med.* 2014; 18: 355–62.
28. **Xiao J.** Cardiac telocytes and fibroblasts in primary culture: different morphologies and immunophenotypes. *PLoS ONE.* 2015; 10: e0115991.
29. **Gherghiceanu M, Popescu LM.** Cardiac telocytes - their junctions and functional implications. *Cell Tissue Res.* 2012; 348: 265–79.
30. **Cretoiu SM, Cretoiu D, Popescu LM.** Human myometrium - the ultrastructural 3D network of telocytes. *J Cell Mol Med.* 2012; 16: 2844–9.
31. **Cismasiu VB, Radu E, Popescu LM.** miR-193 expression differentiates telocytes from other stromal cells. *J Cell Mol Med.* 2011; 15: 1071–4.
32. **Zheng Y, Zhang M, Qian M, et al.** Genetic comparison of mouse lung telocytes with mesenchymal stem cells and fibroblasts. *J Cell Mol Med.* 2013; 17: 567–77.
33. **Sun X, Zheng M, Zhang M, et al.** Differences in the expression of chromosome 1 genes between lung telocytes and other cells: mesenchymal stem cells, fibroblasts, alveolar type II cells, airway epithelial cells and lymphocytes. *J Cell Mol Med.* 2014; 18: 801–10.
34. **Zheng M, Sun X, Zhang M, et al.** Variations of chromosomes 2 and 3 gene expression profiles among pulmonary telocytes, pneumocytes, airway cells, mesenchymal stem cells and lymphocytes. *J Cell Mol Med.* 2014; 18: 2044–60.
35. **Zheng Y, Cretoiu D, Yan G, et al.** Comparative proteomic analysis of human lung telocytes with fibroblasts. *J Cell Mol Med.* 2014; 18: 568–89.
36. **Manetti M, Guiducci S, Ruffo M, et al.** Evidence for progressive reduction and loss of telocytes in the dermal cellular network of systemic sclerosis. *J Cell Mol Med.* 2013; 17: 482–96.
37. **Manetti M, Rosa I, Messerini L, et al.** A loss of telocytes accompanies fibrosis of multiple organs in systemic sclerosis. *J Cell Mol Med.* 2014; 18: 253–62.
38. **Ho YY, Lagares D, Tager AM, et al.** Fibrosis – a lethal component of systemic sclerosis. *Nat Rev Rheumatol.* 2014; 10: 390–402.
39. **Mandache E, Gherghiceanu M, Macarie C, et al.** Telocytes in human isolated atrial amyloidosis: ultrastructural remodeling. *J Cell Mol Med.* 2010; 14: 2739–47.
40. **Carneiro SC, Medeiros R, Alves Brollo M, et al.** Dendritic skin cells. *Expert Rev Dermatol.* 2008; 3: 509–15.
41. **Chu CC, Di Meglio P, Nestle FO.** Harnessing dendritic cells in inflammatory skin diseases. *Semin Immunol.* 2011; 23: 28–41.
42. **Ainsworth C.** Immunology: a many layered thing. *Nature.* 2012; 492: S52–4.
43. **Lowes MA, Suárez-Fariñas M, Krueger JG.** Immunology of psoriasis. *Annu Rev Immunol.* 2014; 32: 227–55.
44. **Kim J, Krueger JG.** The immunopathogenesis of psoriasis. *Dermatol Clin.* 2015; 33: 13–23.
45. **Baliwag J, Barnes DH, Johnston A.** Cytokines in psoriasis. *Cytokine.* 2015. pii: S1043-4666(14)00628-0.
46. **Valladeau J, Saeland S.** Cutaneous dendritic cells. *Semin Immunol.* 2005; 17: 273–83.
47. **Wollenberg A.** Inflammatory dendritic epidermal cells wollenberg. In: Ring J, Przybilla B, Ruzicka T, editors. *Handbook of atopic eczema.* Berlin, Heidelberg: Springer; 2006. pp. 288–95.
48. **Zaba LC, Krueger JG, Lowes MA.** Resident and “inflammatory” dendritic cells in human skin. *J Invest Dermatol.* 2009; 129: 302–8.
49. **Klechevsky E, Banchereau J.** Human dendritic cells subsets as targets and vectors for therapy. *Ann NY Acad Sci.* 2013; 1284: 24–30.
50. **Stoitzner P, Pfaller K, Stössel H, et al.** A close-up view of migrating Langerhans cells in the skin. *J Invest Dermatol.* 2002; 118: 117–25.
51. **Romani N, Holzmann S, Tripp CH, et al.** Langerhans cells - dendritic cells of the epidermis. *APMIS.* 2003; 111: 725–40.
52. **Valladeau J.** Langerhans cells. *Med Sci.* 2006; 22: 144–8.
53. **Dziegiel P, Dolińska-Krajewska B, Dumańska M, et al.** Coexpression of CD1a, langerin and Birbeck’s granules in Langerhans cell histiocytoses (LCH) in children: ultrastructural and immunocytochemical studies. *Folia Histochem Cytobiol.* 2007; 45: 21–5.
54. **Sparber F.** Langerhans cells: an update. *J Dtsch Dermatol Ges.* 2014; 12: 1107–11.
55. **Krueger JG, Bowcock A.** Psoriasis pathophysiology: current concepts of pathogenesis. *Ann Rheum Dis.* 2005; 64: ii30–6.
56. **Yoshida K, Kubo A, Fujita H, et al.** Distinct behavior of human Langerhans cells and inflammatory dendritic epidermal cells at tight junctions in patients with atopic derma-

- titis. *J Allergy Clin Immunol.* 2014; 134: 856–64.
57. **Wollenberg A, Wagner M, Günther S, et al.** Plasmacytoid dendritic cells: a new cutaneous dendritic cell subset with distinct role in inflammatory skin diseases. *J Invest Dermatol.* 2002; 119: 1096–102.
 58. **Gregorio J, Meller S, Conrad C, et al.** Plasmacytoid dendritic cells sense skin injury and promote wound healing through type I interferons. *J Exp Med.* 2010; 207: 2921–30.
 59. **Glitzner E, Korosec A, Brunner PM, et al.** Specific roles for dendritic cell subsets during initiation and progression of psoriasis. *EMBO Mol Med.* 2014; 6: 1312–27.
 60. **Rusu MC, Jianu AM, Mirancea N, et al.** Tracheal telocytes. *J Cell Mol Med.* 2012; 16: 401–5.
 61. **Cantarero Carmona I, Luesma Bartolomé MJ, Junquera Escribano C.** Identification of telocytes in the lamina propria of rat duodenum: transmission electron microscopy. *J Cell Mol Med.* 2011; 15: 26–30.
 62. **Zheng Y, Bai C, Wang X.** Potential significance of telocytes in the pathogenesis of lung diseases. *Expert Rev Respir Med.* 2012; 6: 45–9.
 63. **Cretoiu D, Cretoiu SM, Simionescu AA, et al.** Telocytes, a distinct type of cell among the stromal cells present in the lamina propria of jejunum. *Histol Histopathol.* 2012; 27: 1067–78.
 64. **Heidenreich R, Röcken M, Ghoreschi K.** Angiogenesis: the new potential target for the therapy of psoriasis? *Drug News Perspect.* 2008; 21: 97–105.
 65. **Heidenreich R, Röcken M, Ghoreschi K.** Angiogenesis drives psoriasis pathogenesis. *Int J Exp Pathol.* 2009; 90: 232–48.
 66. **Chua RA, Arbiser JL.** The role of angiogenesis in the pathogenesis of psoriasis. *Autoimmunity.* 2009; 42: 574–9.
 67. **Berrios RL, Arbiser JL.** Novel antiangiogenic agents in dermatology. *Arch Biochem Biophys.* 2011; 508: 222–6.
 68. **Li W, Man XY, Chen JQ, et al.** Targeting VEGF/VEGFR in the treatment of psoriasis. *Discov Med.* 2014; 18: 97–104.
 69. **Manole CG, Cismaşiu V, Gherghiceanu M, et al.** Experimental acute myocardial infarction: telocytes involvement in neo-angiogenesis. *J Cell Mol Med.* 2011; 15: 2284–96.
 70. **Abramoff MD, Magalhaes PJ, Ram SJ.** Image processing with ImageJ. *Biophotonics International.* 2004; 11: 36–42.
 71. **Micali G, Lacarrubba F, Musumeci ML, et al.** Cutaneous vascular patterns in psoriasis. *Int J Dermatol.* 2010; 49: 249–56.
 72. **Braverman IM.** The cutaneous microcirculation. *J Investig Dermatol Symp Proc.* 2000; 5: 3–9.
 73. **Hern S, Stanton AW, Mellor R, et al.** Control of cutaneous blood vessels in psoriatic plaques. *J Invest Dermatol.* 1999; 113: 127–32.
 74. **Rensen SS, Doevendans PA, van Eys GJ.** Regulation and characteristics of vascular smooth muscle cell phenotypic diversity. *Neth Heart J.* 2007; 15: 100–8.
 75. **Campbell JH, Campbell GR.** Smooth muscle phenotypic modulation - a personal experience. *Arterioscler Thromb Vasc Biol.* 2012; 32: 1784–9.